Ajime, TT, Serre, J, Wust, RCI, Burniston, JG, Maes, K, Janssens, W, Troosters, T, Gayan-Ramirez, G and Degens, H

The combination of smoking with vitamin D deficiency impairs skeletal muscle fiber hypertrophy in response to overload in mice

american physiological society

JOURNAL OF APPLIED PHYSIOLOGY

J Appl Physiol 131: 339–351, 2021.
First published June 3, 2021; doi:10.1152/japplphysiol.00733.2020

RESEARCH ARTICLE

The combination of smoking with vitamin D deficiency impairs skeletal muscle fiber hypertrophy in response to overload in mice

Tom Tanjeko Ajime,[1,2,3] Jef Serré,[1] Rob C. I. Wüst,[4] Jatin G. Burniston,[5] Karen Maes,[1] Wim Janssens,[1] Thierry Troosters,[1,2] Ghislaine Gayan-Ramirez,[1]* and Hans Degens[3,6]*

[1]*Laboratory of Respiratory Diseases and Thoracic Surgery, Department of Chronic Diseases and Metabolism, KU Leuven, Leuven, Belgium;* [2]*Research Group for Rehabilitation in Internal Disorders, Department of Rehabilitation Sciences, KU Leuven, Leuven, Belgium;* [3]*Department of Life Sciences, Research Center for Musculoskeletal Science and Sports Medicine, Manchester Metropolitan University, Manchester, United Kingdom;* [4]*Laboratory of Myology, Department of Human Movement Sciences, Faculty of Behavioral and Movement Sciences, Amsterdam Movement Sciences, Vrije Universiteit Amsterdam, Amsterdam, The Netherlands;* [5]*Sport and Exercise Sciences, Liverpool John Moores University, Liverpool, United Kingdom; and* [6]*Department of Health Promotion and Rehabilitation, Lithuanian Sports University, Kaunas, Lithuania*

Abstract

Vitamin D deficiency, which is highly prevalent in the general population, exerts similar deleterious effects on skeletal muscles to those induced by cigarette smoking. We examined whether cigarette smoke (CS) exposure and/or vitamin D deficiency impairs the skeletal muscle hypertrophic response to overload. Male C57Bl/6JolaH mice on a normal or vitamin D-deficient diet were exposed to CS or room air for 18 wk. Six weeks after initiation of smoke or air exposure, sham surgery or denervation of the agonists of the left plantaris muscle was performed. The right leg served as internal control. Twelve weeks later, the hypertrophic response was assessed. CS exposure instigated loss of body and muscle mass, and increased lung inflammatory cell infiltration ($P < 0.05$), independently of diet. Maximal exercise capacity, whole body strength, in situ plantaris muscle force, and key markers of hypertrophic signaling (Akt, 4EBP1, and FoxO1) were not significantly affected by smoking or diet. The increase in plantaris muscle fiber cross-sectional area in response to overload was attenuated in vitamin D-deficient CS-exposed mice (smoking × diet interaction for hypertrophy, $P = 0.03$). In situ fatigue resistance was elevated in hypertrophied plantaris, irrespective of vitamin D deficiency and/or CS exposure. In conclusion, our data show that CS exposure or vitamin D deficiency alone did not attenuate the hypertrophic response of overloaded plantaris muscles, but this hypertrophic response was weakened when both conditions were combined. These data suggest that current smokers who also present with vitamin D deficiency may be less likely to respond to a training program.

NEW & NOTEWORTHY Plantaris hypertrophy caused by compensatory overload after denervation of the soleus and gastrocnemius muscles showed increased mass and fiber dimensions, but to a lesser extent when vitamin D deficiency was combined with cigarette smoking. Fatigue resistance was elevated in hypertrophied plantaris, irrespective of diet or smoking, whereas physical fitness, hypertrophic markers, and in situ plantaris force were similar. These data showed that the hypertrophic response to overload is attenuated when both conditions are combined.

fiber size; hypertrophy; smoking; vitamin D

INTRODUCTION

For several decades, cigarette smoking has remained a major avoidable public health hazard as ~20% of adults worldwide are active cigarette smokers (1). Cigarette smoke (CS) contains more than 5,000 known toxic constituents and several other unidentified components, and it is one of the greatest sources of human exposure to poisonous chemicals (2, 3). CS does not only affect pulmonary function but also has extrapulmonary deleterious effects such as CS-induced skeletal muscle dysfunction (4–8). In humans and animal models, chronic cigarette smoking has been associated with skeletal muscle weakness and atrophy, impaired mitochondrial function, reduced vasodilation, decreased perfusion, and diminished fatigue resistance (6, 9–11).

Skeletal muscle hypertrophy is defined as an increase in muscle mass due to an increase in fiber size (12, 13). It occurs mainly in response to resistance exercise training in humans (14, 15) and in animal models by exercise training, overloading a muscle via denervation (16–23), or elimination of

* G. Gayan-Ramirez and H. Degens contributed equally to this work.
Correspondence: H. Degens (h.degens@mmu.ac.uk).
Submitted 25 August 2020 / Revised 25 May 2021 / Accepted 26 May 2021

synergist muscles (24–30). Although denervation of synergists elicits less hypertrophy than synergist ablation (14), the denervation surgery is much less invasive and elicits less inflammation than ablation of synergistic muscles (31).

Skeletal muscle mass and fiber cross-sectional areas are maintained by a tight balance between protein synthesis and degradation, both of which are modulated by physical activity, diet, disease or injury, and hormonal balance, among others (32). CS may impair the skeletal muscle hypertrophic response through its negative effects on muscle protein turnover (9, 33) and its potential to induce systemic inflammation and local muscle hypoxia, which may potentially impair the skeletal muscle hypertrophic response. This has, however, not yet been investigated.

Beside the many functions of vitamin D in metabolism, recent studies in humans and mice have indicated that chronic vitamin D deficiency, which is highly prevalent in the general population, leads to muscle atrophy (particularly in type II fibers), lower strength, lower mitochondrial function, and decreased vitamin D receptor expression (34–37). In addition, vitamin D deficiency may impair muscle regeneration (38) and therefore perhaps also the muscle hypertrophic response to overload. Cigarette smoking has been shown to augment the risk for vitamin D deficiency by impairing the enzymes involved in vitamin D synthesis, increasing the activity of enzymatic markers of liver damage and other mechanisms (39–41). Given that both vitamin D deficiency and cigarette smoking have been associated with muscle wasting and mitochondrial dysfunction, it is perhaps no surprise that a recent study reported that vitamin D deficiency aggravated the muscle wasting induced by cigarette smoking in a mouse model (34). However, whether vitamin D deficiency alone or in combination with cigarette smoking impairs the skeletal muscle hypertrophic response has hitherto not been explored. Better understanding of the interaction may be relevant to human exercise training studies where a weak response to exercise training in ~30% of patients with chronic obstructive pulmonary disease (COPD) remains a poorly understood problem.

The objective of this study was to assess whether cigarette smoking, vitamin D deficiency, or their combination affects the muscle hypertrophic response to overload. To investigate this, we used smoking mice made vitamin D deficient by diet. We hypothesized that *1*) chronic cigarette smoke exposure or vitamin D deficiency blunts the hypertrophic response of skeletal muscle to overload and *2*) this effect is larger when cigarette smoke exposure is combined with vitamin D deficiency. To induce muscle hypertrophy, we overloaded the plantaris muscle through denervation of the gastrocnemius and soleus muscles in one hind limb.

MATERIALS AND METHODS

Study Design

Seventy-two 3-wk-old male C57Bl/6JolaH mice were randomly divided into two groups of 36 mice: one group received a standard diet (wt/wt: 1% calcium and 0.7% phosphorus), whereas the other group received a vitamin D-depleted diet (<200 IU/kg body mass vitamin D) with 20% lactose, 2% calcium, and 1.25% phosphorus to preserve serum calcium and phosphorus homeostasis (34, 42, 43). All mice were housed in an ultraviolet-light-free environment to prevent de novo synthesis of vitamin D in the skin. At the age of 8 wk, mice were subdivided into four groups of 18 mice each: normal diet-air-exposed (NAir), normal diet-smoke-exposed (NSmo), vitamin D-deficient diet-air-exposed (DAir), and vitamin D-deficient diet-smoke-exposed (DSmo) groups. After acclimatization by progressive exposure to cigarette smoke (CS) or room air in soft restrains, the CS-exposed mice were exposed via a nose-only exposure system (InExpose System, SCIREQ, Montreal, Canada) to six 3R4F research cigarettes with filter (Kentucky Tobacco Research and Development Center, University of Kentucky) twice daily, 5 days a week (9, 44) for 18 wk. The air-exposed animals were exposed to room air in soft restrains for the same length of time. After 6 wk of exposure to either room air or CS, the left plantaris muscle was overloaded to induce compensatory hypertrophy (Fig. 1). The model of functional elimination of synergist muscles through denervation of the gastrocnemius and soleus muscles was chosen in this study to overload the plantaris muscle. This model of compensatory hypertrophy of the plantaris muscle is associated with lower inflammation and less-invasive nature of surgery than the ablation model (31), putting a lesser burden on the animal in line with "Refinement" of the three Rs (Replacement, Reduction, and Refinement) to minimize potential pain, suffering, or distress of animals.

Total particle density in CS was measured daily using a particle density meter (Microdust, Casella CEL, Bedford, UK). The average level of total particulate density in CS was 188 ± 29 mg/m^3 during each smoking session. Body mass and food intake were measured weekly using a laboratory balance (KERN Precision balance). Food intake was not measured during the weeks of surgery and recovery.

All experiments were performed in line with the institutional, national, and European guidelines for animal welfare and were approved by the ethical committee for animal experimentation of the KU Leuven (Authorization No. P050/2016).

Induction of Hypertrophy in the Left Plantaris Muscle

The overload of the left plantaris muscle started after 6 wk of cigarette smoke/room air exposure. Mice were anesthetized with a mixture of ketamine (100 mg/kg, Ketalar, Pfizer, Belgium), xylazine (10 mg/kg, Rompun, Bayer, Belgium), and acepromazine (3 mg/kg, Placivet, Kela, Belgium) administered intraperitoneally at a volume of 150 μL/25 g. After cessation of nociceptive responses, an incision was made in the popliteal area of the left hind limb to expose the tibial nerve with blunt dissection. The branches of the tibial nerve that innervate the soleus and gastrocnemius muscles were cut and small segments removed to prevent reinnervation. This strategy imposes an overload and subsequent compensatory hypertrophy of the plantaris muscle (17, 18). A sham operation was performed on the right hind limb that served as an internal control. Postoperative care included intraperitoneal injections of buprenorphine (0.2 mg/kg) once a day for 3 days. After this 3-day recovery, mice were again exposed to either room air or CS.

Physical Fitness

Maximal exercise capacity and whole body strength were measured before the start of CS or room air exposure

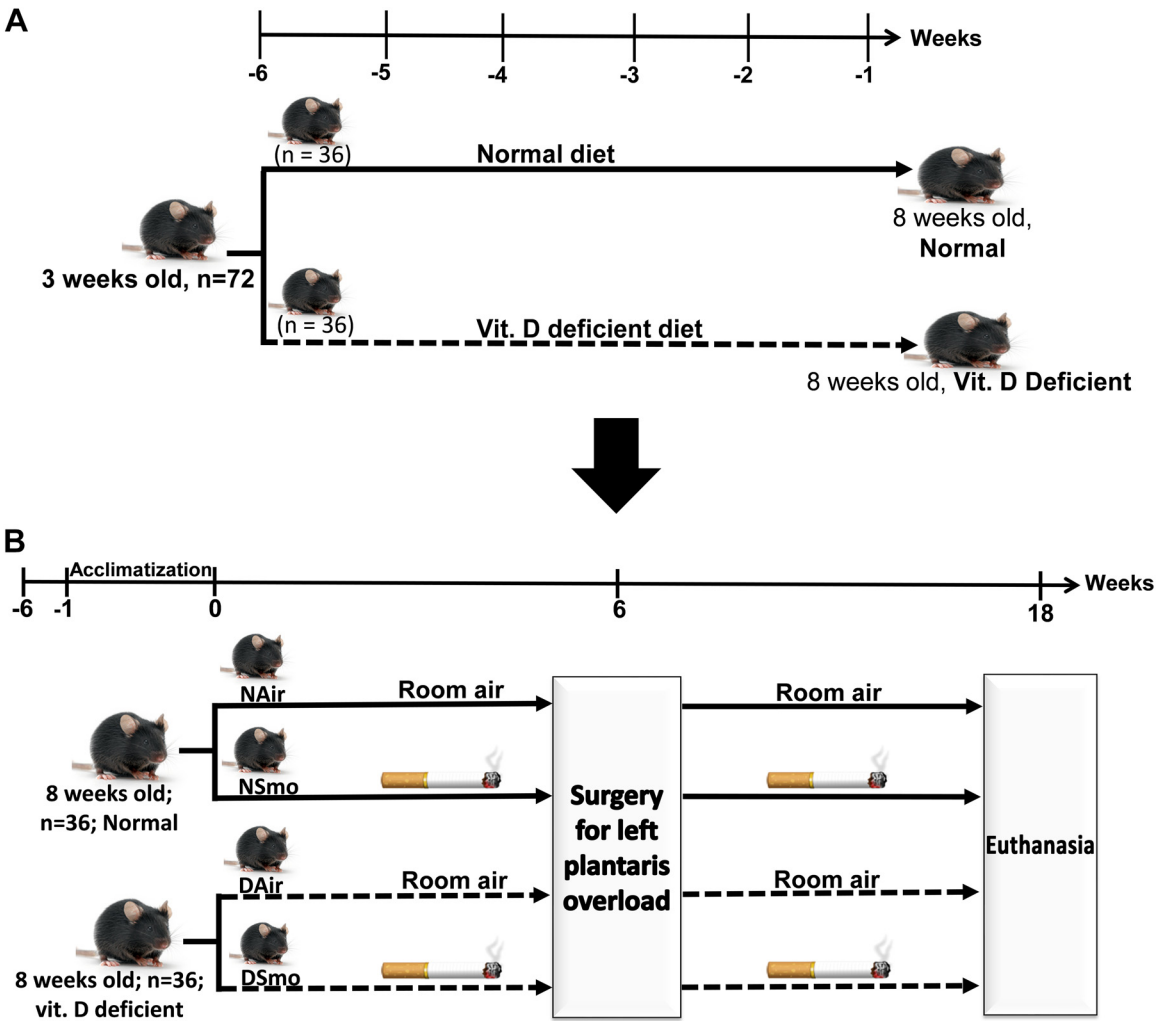

Figure 1. Study design. *A*: seventy-two 3-wk-old male C57Bl/6JolaH mice were randomly assigned to two equal groups and fed for 5 wk with a normal diet or vitamin D-deficient diet. *B*: at the age of 8 wk, the mice were subdivided into four equal groups (n = 18/36) and acclimatized to the setup for 1 wk to be exposed to cigarette smoke (CS) or room air. Surgery to overload the left plantaris muscle was performed 6 wk after starting exposure to CS or room air. Analysis was performed 18 wk after the start of exposure. More details are presented in *Study Design* section. DAir, vitamin D-deficient diet-air-exposed; DSmo, vitamin D-deficient diet-smoke-exposed; NAir, normal diet-air-exposed; NSmo, normal diet-smoke-exposed; vit. D, vitamin D.

(baseline), before surgery (*week 6*), and after 18 wk. The test to measure maximal exercise capacity consisted of a 5-min warm up on a treadmill (0% incline, 3 m/min), followed by 1 m/min increments in speed every minute until exhaustion. Maximal exercise capacity was defined as the maximum speed attained by each animal. Whole body strength was measured by placing the mouse on a grid that was subsequently inverted and the latency-to-fall time was recorded. This served as a proxy for maximal muscle strength.

In Situ Contractile Properties

The force generating capacity and fatigue resistance were determined in situ in the overloaded and sham plantaris muscle, as described before (9, 18). Mice were anaesthetized with a mixture of ketamine (100 mg/kg, Ketalar, Pfizer, Belgium), xylazine (10 mg/kg, Rompun, Bayer, Belgium), and acepromazine (3 mg/kg, Placivet, Kela, Belgium) administered intraperitoneally at a volume of 150 μL/25 g. The plantaris muscle was prepared free, keeping its blood and nerve supply intact, and the distal tendon was attached to a FORT-100 force transducer (World Precision Instruments, Sarasota, FL). The tibial nerve was cut proximally, and the distal end was placed over stimulating electrodes to elicit contractions by supramaximal stimulation. The force was digitally recorded. Optimal muscle length was set with repeated twitch contractions 30 s apart and defined as the length at which maximal active twitch force was developed. The maximal twitch (at 1 Hz) and tetanic (at 200 Hz, train duration = 250 ms) tensions were recorded.

Subsequently, two sequential fatigue resistance tests were performed. The first one, which activates muscle metabolism and blood flow (9, 18), consisted of a 1-min test with 100-Hz contractions with a duty cycle of 100 ms on/1,900 ms off for 1 min (FI100). The second fatigue test consisted of repetitive isometric contractions at 30 Hz with a duty cycle of 330 ms on/670 ms off for 4 min (FI30). Fatigue indices were computed as follows: for FI100, force of the last contraction was divided by the highest contraction in this cycle, whereas for FI30, force 2 min after the strongest contraction was divided by the strongest contraction in this cycle. After the

fatigue test, the optimal length was measured and the plantaris muscle excised and weighed. Forces were reported in mN and as specific force (force normalized to the anatomical cross-sectional area of the muscle). Anatomical cross-sectional area was calculated as follows:

$$\text{Anatomical CSA} = [(\text{muscle mass(g)}]/\{[\text{optimal length (cm)}] \times (1.056\ \text{g/cm}^3)\}, \quad (1)$$

where 1.056 represents the muscle density.

Inflammatory Cell Counts in the Bronchoalveolar Lavage Fluid

To assess lung inflammation, mice were tracheotomized, and the lungs were lavaged four times using Dulbecco's phosphate-buffered saline to obtain bronchoalveolar lavage fluid. Total cell counts were performed with pooled fractions using a hemocytometer (Bürker bright-line, Optic Labor) with trypan blue staining. The rest of the fluid was centrifuged at 1,000 *g* for 10 min at 4°C, and the resulting cell pellets were stained with Diff-Quick (Medical Diagnostics, Düdingen, Germany) and 3×100 cells were counted to obtain differential cell counts (neutrophils, macrophages, and lymphocytes).

Serum Measurements

Serum from blood collected from the vena cava was used to measure 25-OH Vitamin-D3-D6 levels using liquid chromatography-tandem mass spectrometry (LC-MS/MS) (LC, Shimadzu and MS, Qtrap 5500, Sciex) as described previously (44).

Muscle Histology

Left and right plantaris muscles were frozen using isopentane cooled in liquid nitrogen and stored at −80°C. Serial 5-μm cross sections were stained with hematoxylin-eosin to visualize potential structural alterations, and the periodic acid-Schiff (PAS) staining was used to assess glycogen content. To discriminate glycogen from other PAS-positive components (such as glycoproteins and proteoglycans), a serial section per muscle was pretreated with 0.05% α-amylase to digest glycogen and then with PAS, whereas another section was solely stained with PAS. Immunohistochemical staining for myosin heavy chain isoforms was performed on serial sections to measure the fiber cross-sectional areas (FCSA) and fiber type distribution (34). The pooled FCSA was calculated as total FCSA normalized for fiber type distribution. Areal fiber proportions were calculated as (e.g., for type IIA) follows:

$$100\% \times \{(\text{CSA IIA} \times \%\text{IIA})/[(\text{CSA IIA} \times \%\text{IIA}) + (\text{CSA IIX} \times \%\text{IIX}) + (\text{CSA IIB} \times \%\text{IIB})]\}. \quad (2)$$

In each section, 150–180 fibers were analyzed for fiber type composition and FCSA.

Western Immunoblotting of Key Markers of Hypertrophic Signaling

Total protein concentration.

The plantaris muscles were homogenized in Tris-HCl buffer (5 mM EDTA and 5 mM Tris-HCl, pH 7.5) 1:10 (wt/vol) containing a protease inhibitor cocktail (Roche, Complete) as described previously (45). Total protein concentration was measured using the Bradford method and was expressed as μg/mg plantaris weight.

Western blotting.

We performed Western blotting on the overloaded muscles to assess whether there were different expression patterns of the hypertrophic markers between the different groups. For that purpose, equal concentrations of protein (15–30 μg) were separated under reducing conditions using 12% SDS-PAGE (Biorad mini-PROTEAN) and transferred onto polyvinylidene fluoride membranes (Millipore). The membranes were blocked in 5% nonfat dry milk or 5% bovine serum albumin in TBS-0.1% Tween 20 and then incubated overnight at 4°C with primary antibody. The following primary antibodies from Cell Signaling Technologies (Leiden, The Netherlands) were used: anti-phospho-Akt (No. 4060S, 1:2,000), anti-Akt (No. 9272S, 1:2,000), anti-phospho-4EBP1 (No. 2855S, 1:1,000), anti-4EBP1 (No. 9644S, 1:1,000), anti-phospho FoxO1 (No. 9461S, 1:1,000), and anti-FoxO1 (No. 2880S, 1:1,000). After incubation with the horseradish peroxidase (HRP)-conjugated secondary antibody (P0217, Sigma), protein bands were detected using an enhanced chemiluminescence system (Sigma-Aldrich, Belgium and Thermo Fisher Scientific) and analyzed using the software package (Bio 1D) of the blot imaging system (Photo print, Vilber, France), and phosphorylation status (activity) was determined as the ratio of phosphorylated to total protein.

Statistical Analysis

The data were analyzed using GraphPad prism for windows, version 8.2.1 (GraphPad Software, CA) and SPSS statistics v. 26.0 (IBM corporation, NY). A Shapiro–Wilk test was used to test whether the data in each group were normally distributed. Comparison of body mass, whole body strength, maximal exercise capacity, protein levels, and lung inflammation between groups was done using a two-way analysis of variance (ANOVA) with CS exposure and vitamin D deficiency as independent factors. Muscle mass and histology data were analyzed using a three-way ANOVA with CS exposure, vitamin D deficiency, and hypertrophy/atrophy as independent factors. Tukey's post hoc tests were used for multiple comparisons. Mixed-model analysis followed by Tukey's post hoc test was done when the data had random missing values. Multifactor ANOVA was used when the comparison between groups involved more than three variables as was the case with FCSA and proportions. Significance level was set at $P < 0.05$. Values are presented as means ± standard deviation (SD).

RESULTS

Vitamin D Levels in Serum

Serum levels of 25(OH)D in the mice on vitamin D-deficient diet were below the level of detection (<2.1 μg/L) and lower than in the mice on normal diet (19.4 ± 2.8 μg/L). Exposure to CS did not significantly alter the serum vitamin D concentration.

Lung Inflammatory Cell Count

Exposure to CS caused significant lung inflammation as reflected by the higher total cell count, neutrophils, and

macrophages (all $P < 0.0001$) in the bronchoalveolar lavage fluid after smoking, irrespective of diet (Fig. 2, *A–C*).

Body Mass and Food Intake

Body mass increased over time but significantly less in CS-exposed animals from the 11th week on, irrespective of diet (Fig. 3*A*).

Food intake was similar in all groups for the first 2 wk. From *week 3* on, mice on a vitamin D-deficient diet ate less than their counterparts on a normal diet ($P < 0.05$). Also, CS-exposed mice generally ate less than their air-exposed counterparts from *week 5* on ($P < 0.05$). There were no interaction effects (Fig. 3*B*).

Physical Fitness

CS exposure and/or vitamin D deficiency did not significantly affect maximal exercise capacity at any timepoint (Fig. 4*A*). There were also no differences in whole body strength between groups at any timepoint (Fig. 4*B*).

Skeletal Muscle Structure and Contractile Function

Muscle mass.

There was no significant effect of either smoking or vitamin D deficiency on the mass of the control and overloaded plantaris muscle (Fig. 5*A*). As expected, the mass of the overloaded left plantaris muscles was higher than that of the contralateral muscle ($+32\%$, $P < 0.0001$). This response was not significantly affected by CS exposure or vitamin D deficiency (Fig. 5*A*).

The soleus and gastrocnemius (Fig. 5, *B* and *C*) mass in the smoking mice was lower than that of nonsmoking mice, irrespective of diet ($P = 0.012$). The mass of the denervated soleus and gastrocnemius (Fig. 5, *B* and *C*) muscles was lower than the contralateral muscles ($P < 0.0001$), irrespective of group (Fig. 5*B*). The vitamin D × atrophy interaction ($P = 0.008$) for the gastrocnemius muscle was reflected by a larger decrease in muscle mass in vitamin D-deficient mice, irrespective of smoking status (Fig. 5*C*).

Plantaris muscle force and fatigue index.

Despite plantaris hypertrophy, no significant differences were observed in absolute (N) twitch (Fig. 6*A*) and tetanic (Fig. 6*B*) forces compared with the contralateral muscle. The same holds true for specific twitch and tetanic force (Table 1). However, when we compared force measurements from the pooled sham and hypertrophied muscles, not considering the vitamin D or smoking status, we found that the overloaded muscles produced higher absolute twitch ($P = 0.043$) and tetanic ($P = 0.038$) forces than the sham muscles, whereas specific force did not differ significantly (Table 1).

The hypertrophied plantaris muscles had a higher fatigue index (FI100 and FI30) than the contralateral muscle ($P = 0.010$ for FI100 and $P = 0.009$ for FI30, Fig. 6, *C* and *D*) with no significant effect of smoking and/or vitamin D deficiency.

Plantaris Muscle Histology

Compared with sham plantaris muscle, hematoxylin-eosin staining did not show any signs of structural alterations or presence of inflammation in the overload plantaris muscle of any group (Fig. A1). There was also no evidence for glycogen storage in the overload plantaris muscle compared with sham plantaris muscle in any of the groups (Fig. A2).

Plantaris Muscle Fiber Cross-Sectional Area and Fiber Type Composition

Fiber cross-sectional area.

A typical example of a plantaris muscle cross section stained for different myosin heavy chain isoforms used to determine fiber types, areas, and proportions is shown in Fig. 7, *A* and *B*. Due to the low presence or complete absence of type I

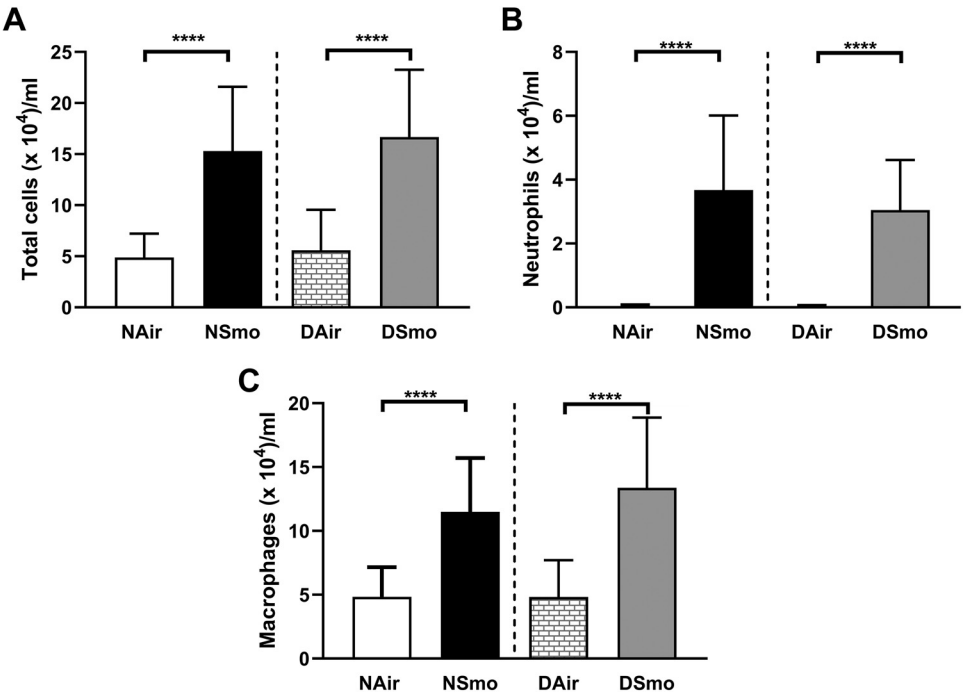

Figure 2. Lung inflammatory cell count. Total cell count (*A*), number of neutrophils (*B*), and macrophages (*C*) were significantly higher in the bronchoalveolar lavage fluid after smoking, irrespective of diet. DAir, vitamin D-deficient diet-air-exposed (brick bars); DSmo, vitamin D-deficient diet-smoke-exposed (gray bars); NAir, normal diet-air-exposed (open bars); NSmo, normal diet-smoke-exposed (black bars) mice. ****$P < 0.0001$. Data are presented as means ± SD.

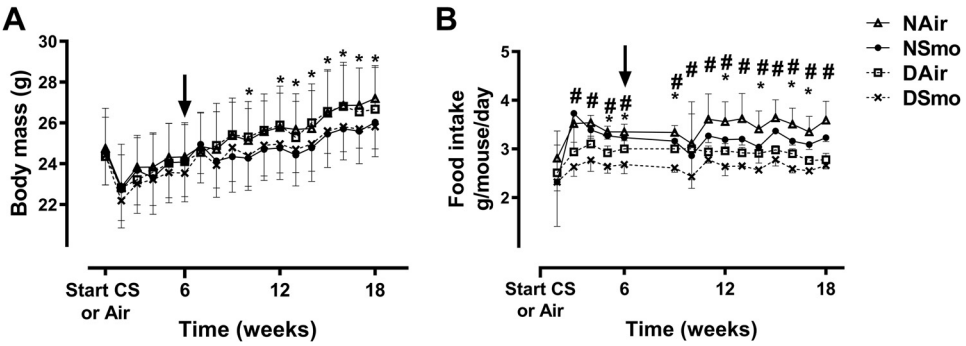

Figure 3. Body mass and food intake during cigarette smoke or air exposure. Body mass gain (*A*) was lower in the cigarette smoke (CS)-exposed mice and food intake (*B*) in vitamin D-deficient mice was less from *week 2*. DAir, vitamin D-deficient diet-air-exposed (open squares); DSmo, vitamin D-deficient diet-smoke-exposed (crosses); NAir, normal diet-air-exposed (open triangles); NSmo, normal diet-smoke-exposed (closed circles) mice. Black arrows indicate overload surgery. $*P < 0.05$ vs. smoking, $\#P < 0.05$ vs. vitamin D deficiency. Values are presented as means ± SD.

muscle fibers in the plantaris, they were not considered in all histological analyses.

The fibers of overloaded plantaris muscles were larger [P = 0.0003 (IIA); P = 0.0002 (IIX); P = 0.0004 (IIB)] compared with the contralateral muscle, when analyzed per type (Fig. 7, *C–E*) or pooled (Fig. 7*F*, P = 0.0016), irrespective of vitamin D deficiency or smoking. However, the increase in FCSA (hypertrophic response) in the vitamin D-deficient smoking mice was smaller (interaction effect between smoking and vitamin D deficiency for hypertrophy; P = 0.03), suggestive of a blunted hypertrophic response in the vitamin D-deficient CS-exposed mice.

Fiber type distribution and areal proportions.

There were no significant main effects of CS exposure, hypertrophy, or vitamin D deficiency on the proportion of type IIA and IIX fibers. However, there were significant interactions between vitamin D deficiency and hypertrophy (P = 0.021) and between CS exposure and hypertrophy (P = 0.038) for the proportion of IIX fibers (Fig. 8*A*), which implies that the combination of vitamin D deficiency and CS exposure led to a higher percentage of IIX fibers in the overloaded muscles but not in the other groups. The numerical (Fig. 8*B*) and areal (Fig. 8*C*) proportions of type IIB fibers were lower in the hypertrophied muscles, irrespective of CS exposure and/or vitamin D deficiency (P = 0.04).

Total protein concentration and protein synthesis markers.

Total protein concentration was similar in the sham and overloaded plantaris, irrespective of smoking or vitamin D status (pooled values: sham 0.153 ± 0.036 μg/mg vs. overload 0.147 ± 0.022 μg/mg plantaris weight).

There were no significant main effects of, or interactions between, CS exposure and vitamin D status on the total protein concentration and activity of Akt (Fig. 9*B*), 4EBP1 (Fig. 9*C*), and FoxO1 (Fig. 9*D*) in the hypertrophied plantaris muscle. Typical examples of Western blots for Akt, phospho-Akt, 4EBP1, phospho-4EBP1, FoxO1, and phospho-FoxO1 can be seen in Fig. 9*A*.

DISCUSSION

This study examined for the first time whether cigarette smoking and/or vitamin D deficiency affect the hypertrophic response of skeletal muscle to overload in mice. Our data reveal that CS exposure or vitamin D deficiency alone did not attenuate muscle fiber hypertrophy in the overloaded plantaris, but this response was reduced in vitamin D-deficient CS-exposed mice. If this can be translated to human application, it might be considered as one possible avenue to explain less training response to resistance training if such patients undergo a training program.

In agreement with previous studies, CS exposure led to significantly lower body mass (4, 8, 9, 46, 47), loss of soleus and gastrocnemius muscle mass (5, 34, 46), and lung inflammatory cell infiltration (47, 48), irrespective of diet. We confirmed that maximal exercise capacity and whole body strength remained unaffected after 14–24 wk of CS exposure (9, 48).

Corresponding with previous studies, mice on the vitamin D-deficient diet became severely deficient as compared with those on a normal diet (44). Even though CS exposure is a known risk factor for vitamin D deficiency (39), it did not alter the levels of vitamin D. Although the mice on a vitamin D-deficient diet generally ate less, their body mass gain was not lower than their counterparts on a normal diet. This

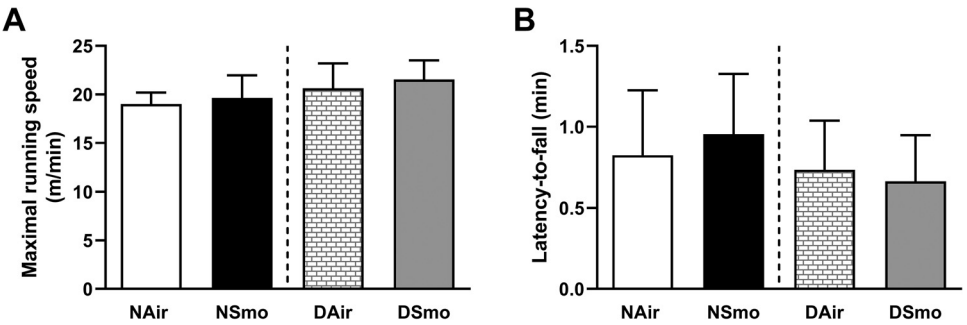

Figure 4. Physical fitness at euthanasia. Maximal exercise capacity (*A*) and whole body strength (latency-to-fall time) (*B*) at euthanasia in all groups. There was no significant difference in maximal exercise capacity or whole body strength between groups. DAir, vitamin D-deficient diet-air-exposed (brick bars); DSmo, vitamin D-deficient diet-smoke-exposed (gray bars); NAir, normal diet-air-exposed (open bars); NSmo, normal diet-smoke-exposed (black bars) mice. Values are presented as means ± SD.

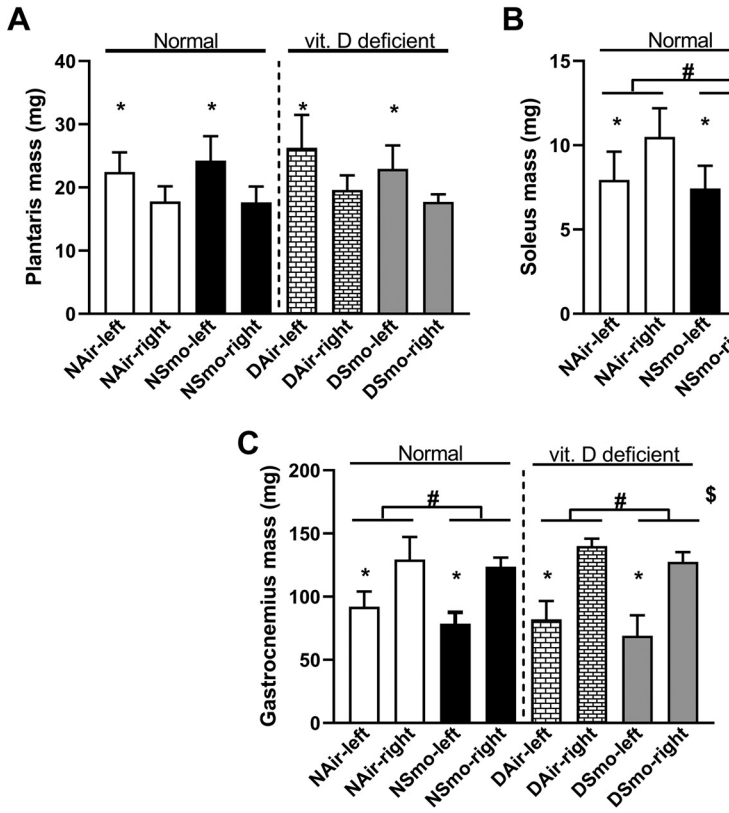

Figure 5. Effects of cigarette smoke exposure, vitamin D deficiency, and overload/denervation on plantaris, soleus, and gastrocnemius muscle mass. Mass of the overloaded (*left*) and sham (*right*) plantaris (*A*), denervated and sham soleus (*B*), and denervated and sham gastrocnemius (*C*). Plantaris muscle overload led to a significant increase in mass, whereas denervation of the soleus and gastrocnemius caused significant decrease in mass. DAir, vitamin D-deficient diet-air-exposed (brick bars); DSmo, vitamin D-deficient diet-smoke-exposed (gray bars); NAir, normal diet-air-exposed (open bars); NSmo, normal diet-smoke-exposed (black bars) mice; vit. D, vitamin D. *Significant hypertrophic or atrophic response ($P < 0.05$); #$P < 0.05$ for air vs. CS; $More atrophy in the gastrocnemius muscles of vitamin D-deficient mice. Values are presented as means ± SD.

suggests that the energy efficiency was elevated or physical activity levels were reduced in mice on a vitamin D-deficient diet. However, the maximal exercise capacity, whole body strength, and skeletal muscle fatigue resistance were not diminished by smoking or vitamin D deficiency. Although all animals underwent a unilateral denervation, and hence most likely had a somewhat altered running gait, these data indicate that the physical activity was not so diminished to

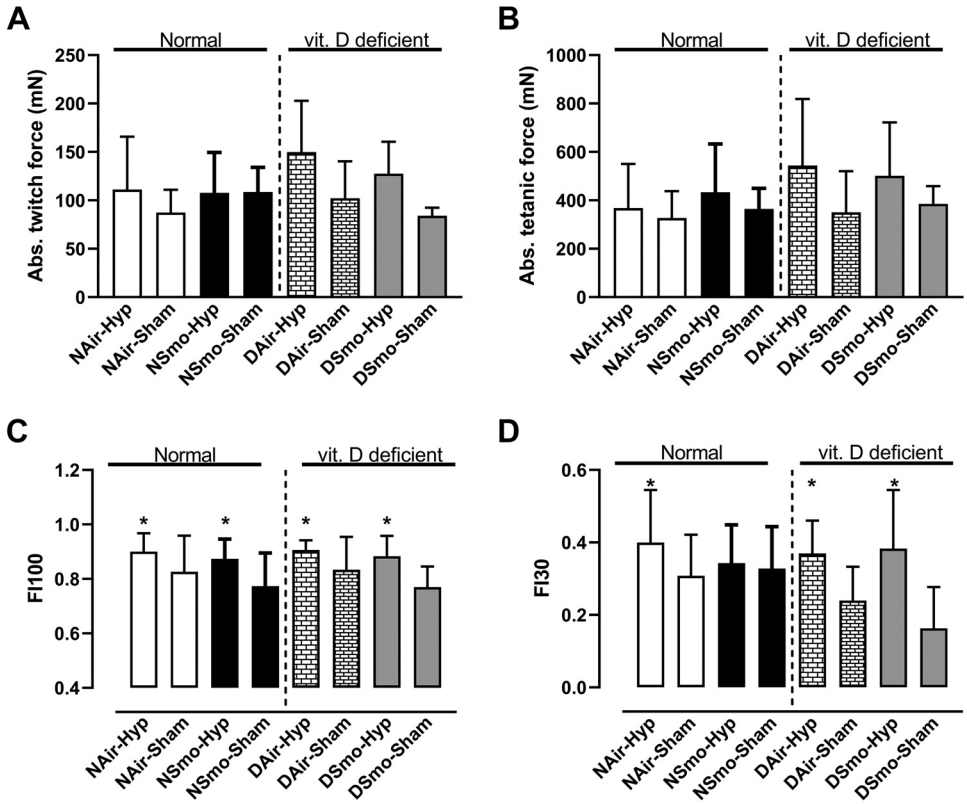

Figure 6. Effects of cigarette smoke exposure and vitamin D deficiency on contractile properties. In situ left hypertrophied (Hyp) and right (Sham) plantaris muscle absolute twitch (1 Hz) force (*A*), absolute tetanic (200 Hz) force (*B*), fatigue index at 100 Hz stimulation (FI100; *C*), and fatigue index at 30 Hz stimulation (FI30; *D*). Hypertrophied plantaris muscles had a higher fatigue resistance, irrespective of diet and/or smoking. Abs., absolute; DAir, vitamin D-deficient diet-air-exposed (brick bars); DSmo, vitamin D-deficient diet-smoke-exposed (gray bars); NAir, normal diet-air-exposed (open bars); NSmo, normal diet-smoke-exposed (black bars) mice; vit. D, vitamin D. *$P < 0.05$ vs. contralateral control. Values are presented as means ± SD.

Table 1. *Specific twitch and tetanic force in vitamin-sufficient (normal) and -deficient mice in the different groups*

	Twitch Force, N/cm^2		Tetanic Force, N/cm^2	
Plantaris Muscle	Normal	Deficient	Normal	Deficient
Air-Hyp	6.3 ± 2.9	7.1 ± 2.2	20.9 ± 10.0	24.9 ± 8.8
Air-Sham	6.3 ± 2.7	6.2 ± 1.7	22.6 ± 6.9	21.1 ± 8.7
Smo-Hyp	5.2 ± 1.8	7.3 ± 1.3	20.6 ± 7.5	28.4 ± 10.5
Smo-Sham	7.3 ± 2.2	6.3 ± 1.0	24.2 ± 4.7	29.0 ± 6.7

Values are presented as means ± SD. Air-Hyp, air-exposed and overload plantaris; Air-Sham, air-exposed and sham plantaris; Smo-Hyp, cigarette smoke-exposed and overload plantaris; Smo-Sham, cigarette smoke-exposed and sham plantaris.

have an impact on skeletal muscle structure and function. In line with this, it has been shown that vitamin D-deficient mice showed no alterations in physical fitness even after 24 wk except when specific muscles were immobilized (49).

In agreement with previous studies reporting muscle wasting due to smoking (48, 50), we also observed a lower muscle mass in smoking mice. Similarly, in our study, there was no significant effect of the vitamin D status on muscle mass in line with previous studies in vitamin D-deficient rats where calcium and phosphorus serum levels were maintained within the normal range (51, 52). Another factor that may underlie the muscle wasting in these conditions is disuse as suggested by the reduced exercise capacity in vitamin D deficiency (53), although the mice in our and another study (49) showed no indication of reduced exercise capacity.

As expected, overload of the left plantaris muscle by denervation of synergists in our study led to hypertrophy as demonstrated by the increase in plantaris mass and FCSA. Although CS exposure and/or vitamin D deficiency alone did not attenuate the compensatory increase in plantaris mass and fiber size, combination of smoking and vitamin D deficiency reduced the overload-induced fiber hypertrophy. It

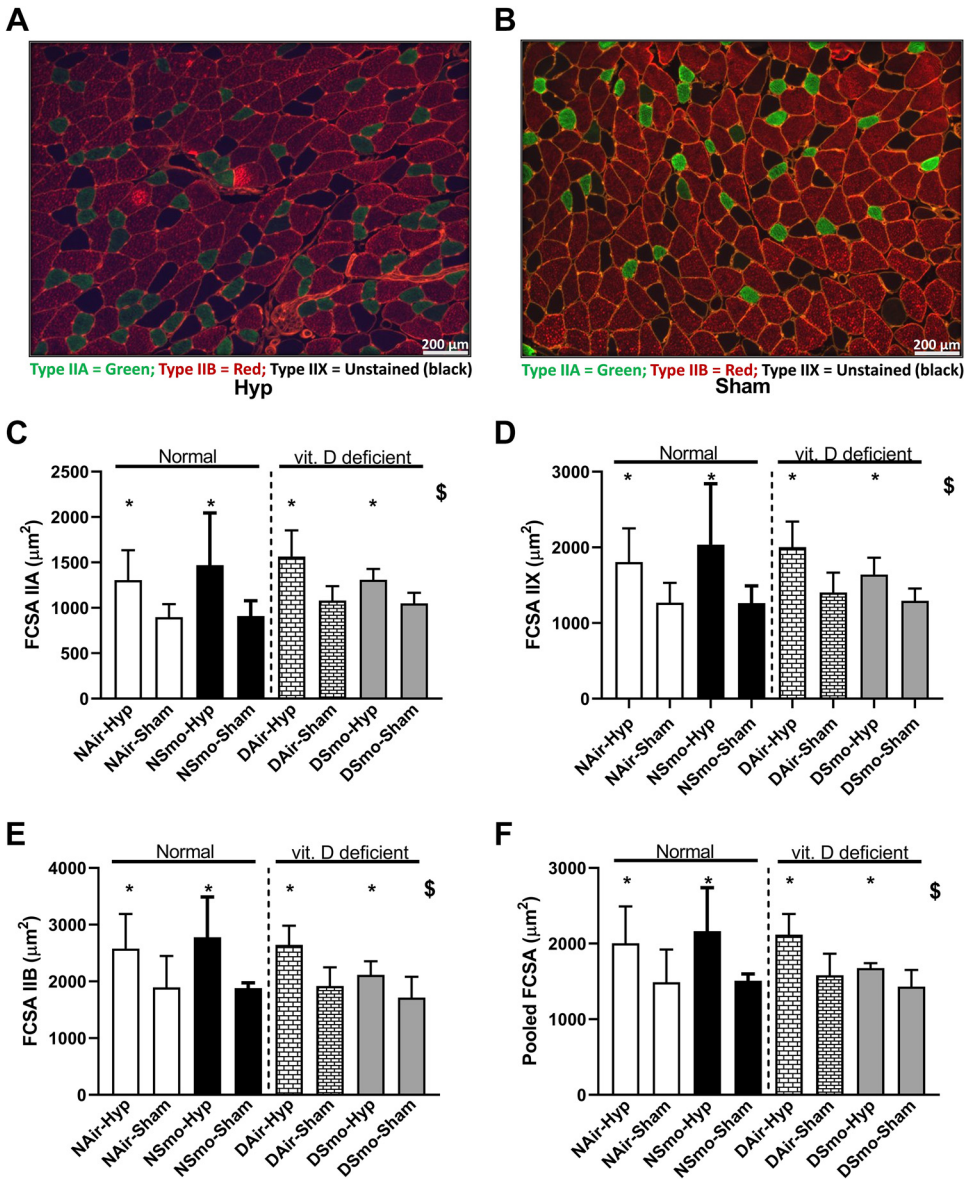

Figure 7. Effects of cigarette smoke exposure, vitamin D deficiency, and overload on plantaris muscle fiber cross-sectional area (FCSA). Representative example of left hypertrophied (Hyp) (*A*) and right (Sham) (*B*) plantaris muscle cross sections stained for the different myosin heavy chain isoforms. IIA (*C*), IIX (*D*), IIB (*E*), and pooled (*F*) fiber cross-sectional areas (FCSA) in Hyp and sham plantaris in DAir, vitamin D-deficient diet-air-exposed (brick bars); DSmo, vitamin D-deficient diet-smoke-exposed (gray bars); NAir, normal diet-air-exposed (open bars); NSmo, normal diet-smoke-exposed (black bars) mice. Hypertrophy led to an increase in FCSA, irrespective of diet or smoking. *Significant effect of hypertrophy ($P < 0.05$ vs. contralateral control); $Blunted hypertrophic response in vitamin D-deficient CS-exposed mice ($P < 0.05$). Values are presented as means ± SD. vit. D, vitamin D.

J Appl Physiol • doi:10.1152/japplphysiol.00733.2020 • www.jap.org

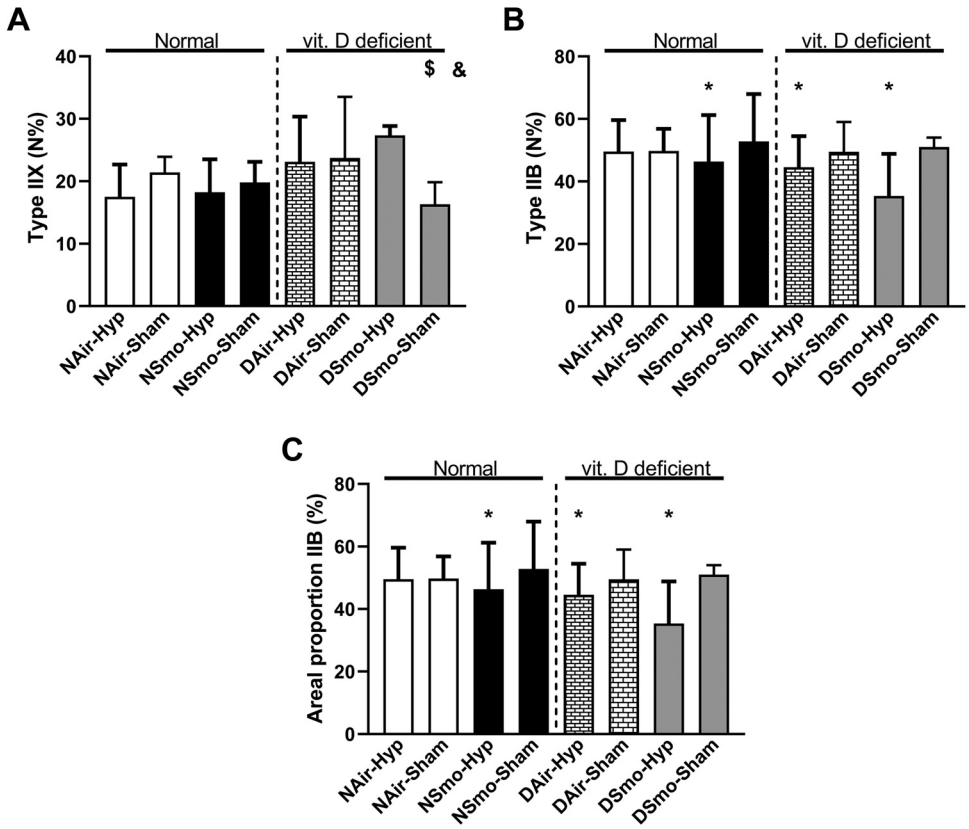

Figure 8. Fiber proportions and contribution to total area. Numerical proportions of type IIX (*A*), IIB (*B*), and areal proportions of IIB (*C*) fibers in the hypertrophied (Hyp) and sham plantaris muscle in DAir, vitamin D-deficient diet-air-exposed (brick bars); DSmo, vitamin D-deficient diet-smoke-exposed (gray bars); NAir, normal diet-air-exposed (open bars); NSmo, normal diet-smoke-exposed (black bars) mice. The hypertrophied plantaris muscle had a lower numerical and areal proportion of type IIB fibers, whereas type IIX fiber proportions only showed interactions (vitamin D deficiency × hypertrophy; CS-exposure × hypertrophy) with no main effects of CS exposure, hypertrophy, or vitamin D deficiency. *Significant effect of hypertrophy ($P < 0.05$ vs. contralateral control); $Larger overload effect compared with CS exposure ($P = 0.038$); &Larger overload effect compared with vitamin D deficiency. The interactions suggest that combined treatment caused lower %IIX. Values are presented as means ± SD. vit. D, vitamin D.

might be possible that an overload model, like synergist ablation that induces a larger amount of hypertrophy than denervation of synergists (14), would have shown a more profound inhibition of the hypertrophic response. Despite the attenuated fiber hypertrophy, the smoking vitamin D-deficient mice showed no attenuated increase in muscle mass. This apparent dissociation between muscle fiber hypertrophy and the increase in muscle mass may be attributable to measuring errors in muscle mass that were proportionally larger for smaller than larger muscle masses and/or a type II statistical error. Whatever the cause, the findings of the attenuated fiber hypertrophy in smoking and vitamin D-deficient mice give an indication that current smokers who also present with vitamin D deficiency may be less likely to respond to a training program.

Despite the overload-induced increase in plantaris muscle mass and FCSA, there were no significant changes in plantaris force-generating capacity, irrespective of CS exposure and/or vitamin D deficiency. Although the plantaris muscle was not stronger, it is unlikely that the hypertrophy was related to inflammation, as inflammation has been shown to occur within the first week of overload only (28, 54, 55), and the model we used is associated with less inflammation than ablation of synergists (31). This is further confirmed in our study by the absence of signs of inflammation in hematoxylin-eosin-stained muscle sections. In addition, hypertrophy was probably not related to water retention due to glycogen, as the glycogen content appeared similar in sham and overloaded muscles. Perhaps the most convincing argument against any pseudohypertrophy is the similar specific tension in sham and overloaded muscles, a consistent observation in this model of overload by denervation of synergist muscles (16, 20, 23), whereas ablation is often accompanied by a reduction in specific tension (26, 56). There were, however, no significant interactions with vitamin D or smoking status, and when all data were pooled, not considering smoking or vitamin D status, hypertrophy was associated with an increase in force-generating capacity. This overload-induced increase in force-generating capacity is in line with previous studies in both rats on a normal diet (19) and mice (17, 23, 26).

The hypertrophied plantaris muscles of the mice in our study were more resistant to fatigue, irrespective of CS exposure and/or vitamin D deficiency. This improved fatigue resistance may be the result of a decreased proportion of type IIB fibers as observed here and by others (22, 57), as the ATP cost for isometric tension is higher for type IIB than any other fiber type (58). Thus, although the hypertrophic response was blunted in the presence of both vitamin D deficiency and smoking, this combination did not attenuate the improvement in fatigue resistance during hypertrophy.

To determine whether there was a different expression pattern of the hypertrophic markers in the overloaded plantaris depending on whether the animals were smokers or vitamin D deficient or sufficient, key markers of hypertrophic signaling pathways were measured in the hypertrophied plantaris muscles. No differences in protein levels of positive regulators (Akt and 4EBP1) (57) and negative regulators (FoxO1) (59) of muscle protein homeostasis were observed between the different groups, indicating no effect of CS and/or vitamin D deficiency on these hypertrophic markers within the overload plantaris. The lack of differences in the levels of hypertrophic

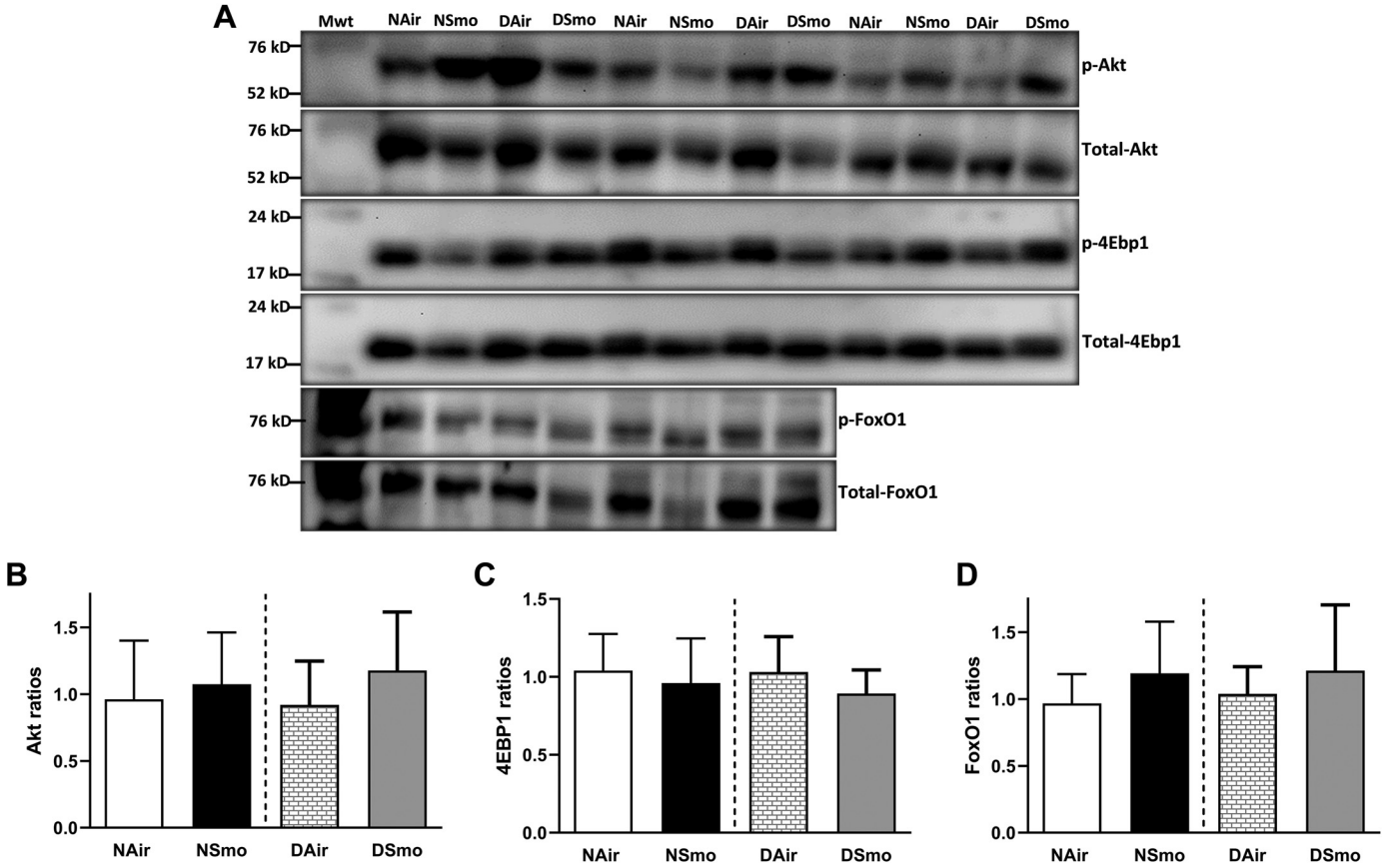

Figure 9. Protein synthesis markers in left plantaris. *A*: representative examples of Western immunoblots from hypertrophied plantaris muscles for phospho-Akt, total-Akt, phospho-4EBP1, total-4EBP1, phospho-FoxO1, and total-FoxO1. Phospho-Akt/total-Akt ratios (*B*), phospho-4EBP1/total-4EBP1 ratios (*C*), and phospho-FoxO1/total-FoxO1 ratios (*D*) in DAir, vitamin D-deficient diet-air-exposed (brick bars); DSmo, vitamin D-deficient diet-smoke-exposed (gray bars); NAir, normal diet-air-exposed (open bars); NSmo, normal diet-smoke-exposed (black bars) mice. There were no significant effects of cigarette smoking or vitamin D status. Values are presented as means ± SD.

markers in our study might reflect that the increase in these hypertrophic markers is of a similar magnitude in the different groups and/or that we were too late in the time course of the development of hypertrophy to still be able to detect activation of the hypertrophic signaling pathways. Indeed, the activation of hypertrophic signaling pathways during overload is a transient phenomenon, with enhanced hypertrophic markers occurring during the first 3 wk after overload to then normalizing to control levels. For instance, it has been reported that IGF-1, mechanosensitive growth factor (MGF), and myogenin remained elevated for 2–4 wk after induction of plantaris overload (24, 25) to then return to baseline levels (24). Similarly, phosphorylation of 4EBP1 remained elevated 15 days after overload and had returned to control levels by 90 days (24), and phosphorylation of Akt was reported 2–10 days after overload (27) and had returned to baseline values after 14 days of overload (26). Our data on unchanged 4EBP1 and Akt 12 wk (84 days) in the overload muscles are, therefore, not completely surprising and would support the interpretation of being too late to still detect activation of hypertrophic signaling. However, it may well be possible that the hypertrophic response was somewhat delayed during smoking or vitamin D deficiency as a consequence of an attenuated activation of these signaling pathways, but with our study design, we did not catch this event. Such a situation is reminiscent to the delayed response to electrical stimulation in muscles (60) and the delayed hypertrophy after reloading of disused muscle (61) from old rodents. It therefore remains to be seen whether the development of hypertrophy is delayed in vitamin D deficiency and/or smoking.

We can, however, not entirely exclude that these markers were elevated in the overloaded muscles, as the expression was solely determined in the overload and not in the corresponding sham plantaris muscles. Admittedly, if we also had the data for the sham legs, we could have determined whether the markers were elevated in the hypertrophied muscles. Nevertheless, the expression levels of these markers were similar in the hypertrophic muscles of the different groups, suggesting that at least after 84 days of overload, there is indeed no indication of a different response to overload of these markers in the different groups.

To conclude, even though smoking and vitamin D deficiency individually did not alter the hypertrophic response of skeletal muscle to overload, the combination of smoking and vitamin D deficiency did blunt the development of overload-induced hypertrophy. These findings should be kept in mind especially when attempting to improve muscle mass in individuals who are smoking and vitamin D deficient.

APPENDIX

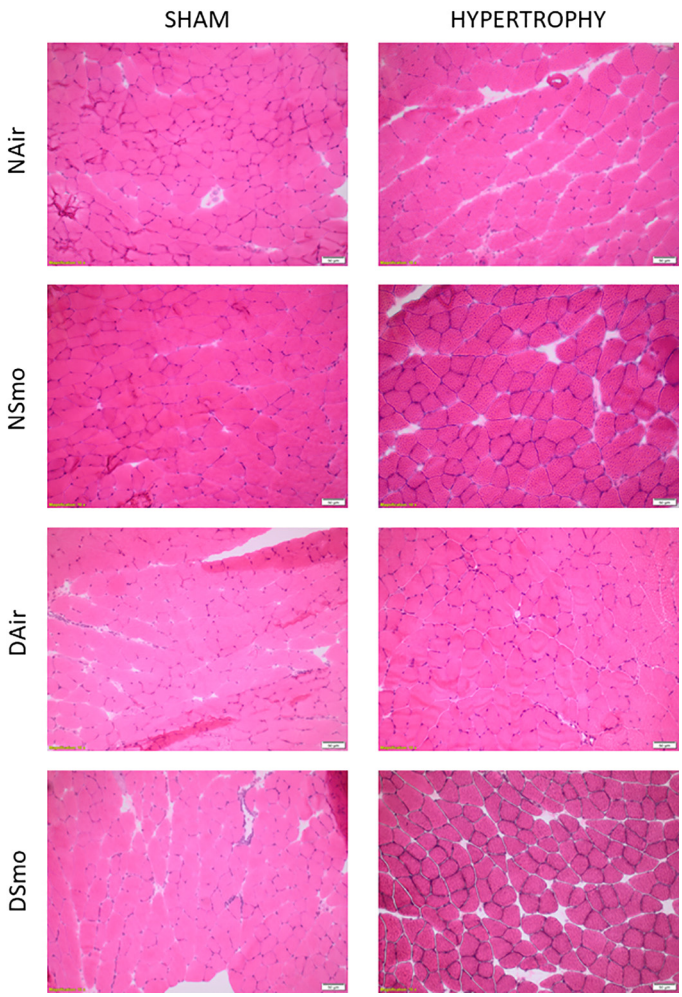

Figure A1. Hematoxylin-eosin staining of sham (*left*) and hypertrophied (*right*) plantaris in vitamin-sufficient (normal) and -deficient mice in the different groups. DAir, vitamin D-deficient diet-air-exposed; DSmo, vitamin D-deficient diet-smoke-exposed; NAir, normal diet-air exposed; NSmo, normal diet-smoke-exposed mice. Scale represents 50 μm.

DATA AVAILABILITY

The data that support the findings of this study are available from the corresponding author upon reasonable request.

GRANTS

This study was funded by the Directorate-General for Education and Culture of the European Commission through MOVE-AGE, Erasmus Mundus Joint Doctorate in prevention of loss of mobility with ageing (2011–2015).

DISCLOSURES

No conflicts of interest, financial or otherwise, are declared by the authors.

AUTHOR CONTRIBUTIONS

A.T.T., W.J., T.T., G.G-R., and H.D. conceived and designed research; A.T.T., J.S., K.M., G.G-R., and H.D. performed experiments; A.T.T., R.C.I.W., K.M., T.T., G.G-R., and H.D. analyzed data; A.T.T., J.S., R.C.I.W., K.M., T.T., G.G-R., and H.D. interpreted results of experiments; A.T.T. prepared figures; A.T.T., J.S., R.C.I.W., G.G-R., and H.D. drafted manuscript; A.T.T., J.S., R.C.I.W., J.G.B., K.M., W.J., T.T., G.G-R., and H.D. edited and revised manuscript; A.T.T., J.S., R.C.I.W., J.G.B., K.M., W.J., T.T., G.G-R., and H.D. approved final version of manuscript.

REFERENCES

1. **Basu S**, **Stuckler D**, **Bitton A**, **Glantz SA.** projected effects of tobacco smoking on worldwide tuberculosis control: mathematical modelling analysis. *BMJ* 343: d5506–d5511, 2011. doi:10.1136/bmj.d5506.
2. **Smith CJ**, **Fischer TH.** Particulate and vapor phase constituents of cigarette mainstream smoke and risk of myocardial infarction. *Atherosclerosis* 158: 257–267, 2001. doi:10.1016/S0021-9150(01)00570-6.
3. **Swan GE**, **Lessov-Schlaggar CN.** The effects of tobacco smoke and nicotine on cognition and the brain. *Neuropsychol Rev* 17: 259–273, 2007. doi:10.1007/s11065-007-9035-9.
4. **Barreiro E**, **del Puerto-Nevado L**, **Puig-Vilanova E**, **Pérez-Rial S**, **Sánchez F**, **Martínez-Galán L**, **Rivera S**, **Gea J**, **González-Mangado N**, **Peces-Barba G.** Cigarette smoke-induced oxidative stress in skeletal muscles of mice. *Respir Physiol Neurobiol* 182: 9–17, 2012. doi:10.1016/j.resp.2012.02.001.
5. **Caron M-A**, **Morissette MC**, **Thériault M-E**, **Nikota JK**, **Stämpfli MR**, **Debigaré R.** Alterations in skeletal muscle cell homeostasis in a mouse model of cigarette smoke exposure. *PLoS One* 8: e66433, 2013. doi:10.1371/journal.pone.0066433.
6. **Degens H**, **Gayan-Ramirez G**, **Van Hees HWH.** Smoking-induced skeletal muscle dysfunction: from evidence to mechanisms. *Am J Respir Crit Care Med* 191: 620–625, 2015. doi:10.1164/rccm.201410-1830PP.
7. **Liu Q**, **Xu WG**, **Luo Y**, **Han FF**, **Yao XH**, **Yang TY**, **Zhang Y**, **Pi WF**, **Guo XJ.** Cigarette smoke-induced skeletal muscle atrophy is associated with up-regulation of USP-19 via p38 and ERK MAPKs. *J Cell Biochem* 112: 2307–2316, 2011. doi:10.1002/jcb.23151.
8. **Tang K**, **Wagner PD**, **Breen EC.** TNF-alpha-mediated reduction in PGC-1alpha may impair skeletal muscle function after cigarette smoke exposure. *J Cell Physiol* 222: 320–327, 2010. doi:10.1002/jcp.21955.
9. **Ajime TT**, **Serré J**, **Wüst RCI**, **Messa GAM**, **Poffé C**, **Swaminathan A**, **Maes K**, **Janssens W**, **Troosters T**, **Degens H**, **Gayan-Ramirez G.** Two weeks of smoking cessation reverse cigarette smoke-induced skeletal muscle atrophy and mitochondrial dysfunction in mice. *Nicotine Tob Res* 23: 143–151, 2021. doi:10.1093/ntr/ntaa016.
10. **Ciftci Ö**, **Günday M**, **Caliskan M**, **Güllü H**, **Güven A**, **Müderrisoglu H.** Light cigarette smoking and vascular function. *Acta Cardiol* 68: 255–261, 2013. doi:10.2143/AC.68.3.2983419.
11. **Wüst RCI**, **Jaspers RT**, **van der Laarse WJ**, **Degens H.** Skeletal muscle capillarization and oxidative metabolism in healthy smokers. *Appl Physiol Nutr Metab* 33: 1240–1245, 2008. doi:10.1139/H08-116.
12. **Gollnick PD**, **Timson BF**, **Moore RL**, **Riedy M.** Muscular enlargement and number of fibers in skeletal muscles of rats. *J Appl Physiol Respir Environ Exerc Physiol* 50: 936–943, 1981. doi:10.1152/jappl.1981.50.5.936.
13. **Russell B**, **Motlagh D**, **Ashley WW.** Form follows function: how muscle shape is regulated by work. *J Appl Physiol (1985)* 88: 1127–1132, 2000. doi:10.3168/jds.2013-7450.
14. **Degens H.** Determinants of skeletal muscle hypertrophy and the attenuated hypertrophic response at old age. *J Sport Medic Doping Studie* S1: 003, 2012. doi:10.4172/2161-0673.S1-003.
15. **Folland JP**, **Williams AG.** The adaptations to strength training: morphological and neurological contributions to increased strength. *Sports Med* 37: 145–168, 2007. doi:10.2165/00007256-200737020-00004.
16. **Ballak SB**, **Busé-Pot T**, **Harding PJ**, **Yap MH**, **Deldicque L**, **de Haan A**, **Jaspers RT**, **Degens H.** Blunted angiogenesis and hypertrophy are associated with increased fatigue resistance and unchanged aerobic capacity in old overloaded mouse muscle. *Age (Dordr)* 38: 39, 2016. doi:10.1007/s11357-016-9894-1.

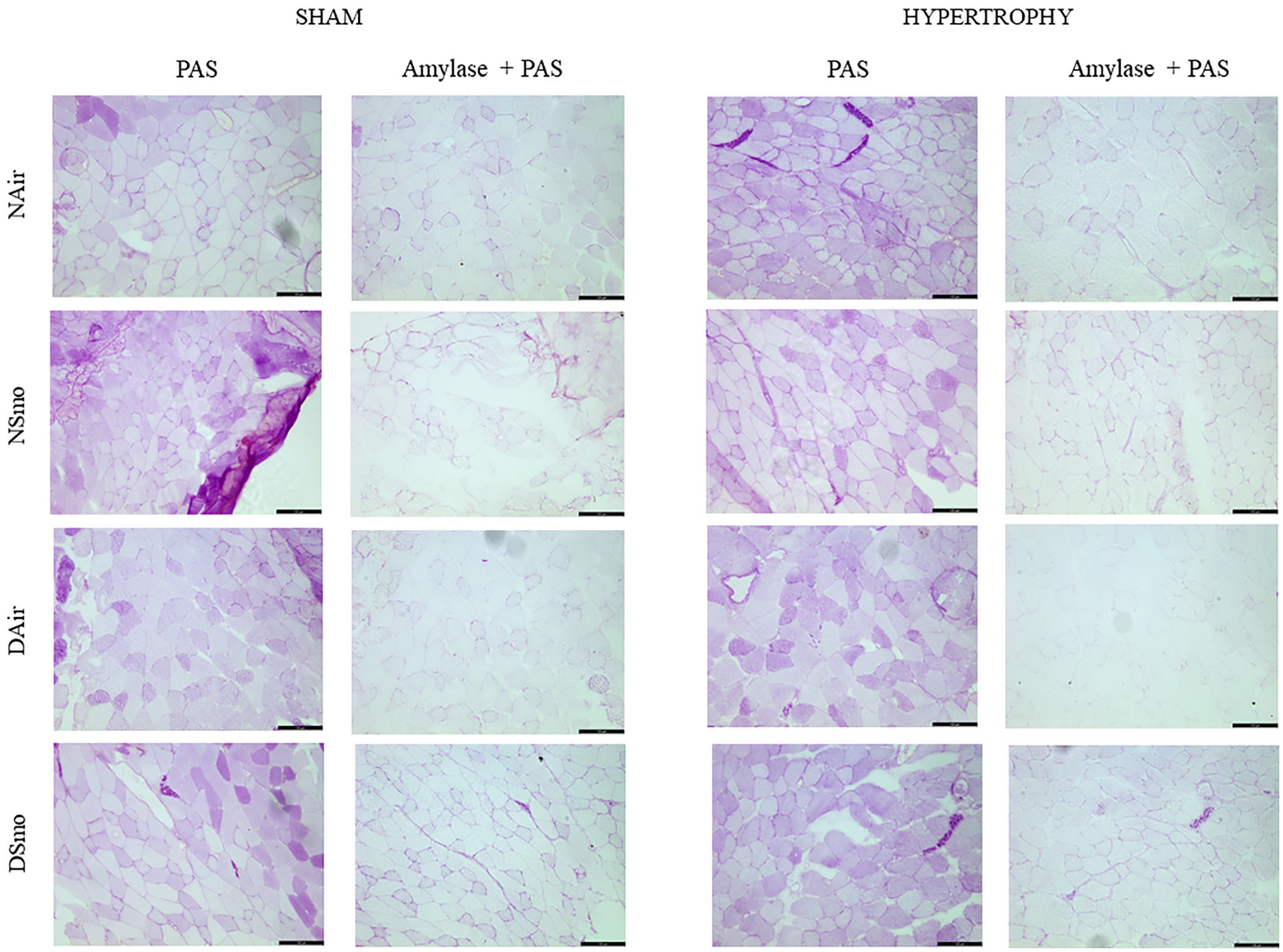

Figure A2. Periodic acid-Schiff (PAS) staining with pretreatment with amylase of sham and hypertrophied plantaris in vitamin-sufficient (normal) and -deficient mice in the different groups. DAir, vitamin D-deficient diet-air-exposed; DSmo, vitamin D-deficient diet-smoke-exposed; NAir, normal diet-air exposed; NSmo, normal diet-smoke-exposed mice. Scale represents 100 μm.

17. **Ballak SB**, **Jaspers RT**, **Deldicque L**, **Chalil S**, **Peters EL**, **de Haan A**, **Degens H.** Blunted hypertrophic response in old mouse muscle is associated with a lower satellite cell density and is not alleviated by resveratrol. *Exp Gerontol* 62: 23–31, 2015. doi:10.1016/j.exger.2014.12.020.
18. **Degens H**, **Alway SE.** Skeletal muscle function and hypertrophy are diminished in old age. *Muscle Nerve* 27: 339–347, 2003. doi:10.1002/mus.10314.
19. **Degens H**, **Hoofd L**, **Binkhorst RA.** Specific force of the rat plantaris muscle changes with age, but not with overload. *Mech Ageing Dev* 78: 215–219, 1995. doi:10.1016/0047-6374(94)01538-W.
20. **Degens H**, **Meessen NEL**, **Wirtz P**, **Binkhorst RA.** The development of compensatory hypertrophy in the plantaris muscle of the rat. *Ann Anat* 177: 285–289, 1995. doi:10.1016/S0940-9602(11)80203-7.
21. **Degens H**, **Turek Z**, **Hoofd LJ**, **Van't Hof MA**, **Binkhorst RA.** The relationship between capillarisation and fibre types during compensatory hypertrophy of the plantaris muscle in the rat. *J Anat* 180: 455–463, 1992.
22. **Degens H**, **Veerkamp JH**, **Van Moerkerk HTB**, **Turek Z**, **Hoofd LJC**, **Binkhorst RA.** Metabolic capacity, fibre type area and capillarization of rat plantaris muscle. Effects of age, overload and training and relationship with fatigue resistance. *Int J Biochem* 25: 1141–1148, 1993. doi:10.1016/0020-711X(93)90592-3.
23. **Hendrickse PW**, **Krusnauskas R**, **Hodson-Tole E**, **Venckunas T**, **Degens H.** Endurance exercise plus overload induces fatigue resistance and similar hypertrophy in mice irrespective of muscle mass. *Exp Physiol* 105: 2110–2122, 2020. doi:10.1113/ep089096.
24. **Adams GR**, **Caiozzo VJ**, **Haddad F**, **Baldwin KM.** Cellular and molecular responses to increased skeletal muscle loading after irradiation. *Am J Physiol Cell Physiol* 283: C1182–C1195, 2002. doi:10.1152/ajpcell.00173.2002.
25. **Adams GR**, **Haddad F.** The relationships among IGF-1, DNA content, and protein accumulation during skeletal muscle hypertrophy. *J Appl Physiol (1985)* 81: 2509–2516, 1996. doi:10.1152/jappl.1996.81.6.2509.
26. **Huey KA**, **Smith SA**, **Sulaeman A**, **Breen EC.** Skeletal myofiber VEGF is necessary for myogenic and contractile adaptations to functional overload of the plantaris in adult mice. *J Appl Physiol (1985)* 120: 188–195, 2016. doi:10.1152/japplphysiol.00638.2015.
27. **Miyazaki M**, **Mccarthy JJ**, **Fedele MJ**, **Esser KA.** Early activation of mTORC1 signalling in response to mechanical overload is independent of phosphoinositide 3-kinase/Akt signalling. *J Physiol* 589: 1831–1846, 2011. doi:10.1113/jphysiol.2011.205658.
28. **Novak ML**, **Billich W**, **Smith SM**, **Sukhija KB**, **McLoughlin TJ**, **Hornberger TA**, **Koh TJ.** COX-2 inhibitor reduces skeletal muscle hypertrophy in mice. *Am J Physiol Regul Integr Comp Physiol* 296: R1132–R1139, 2009. doi:10.1152/ajpregu.90874.2008.
29. **Roy RR**, **Edgerton VR.** Response of mouse plantaris muscle to functional overload: comparison with rat and cat. *Comp Biochem Physiol Part A Physiol* 111: 569–575, 1995. doi:10.1016/0300-9629(95)00062-C.

30. **Stantzou A**, **Relizani K**, **Morales-Gonzalez S**, **Gallen C**, **Grassin A**, **Ferry A**, **Schuelke M**, **Amthor H.** Extracellular matrix remodelling is associated with muscle force increase in overloaded mouse plantaris muscle. *Neuropathol Appl Neurobiol* 47: 218–235, 2021. doi:10.1111/nan.12655.
31. **Lowe DA**, **Alway SE.** Animal models for inducing muscle hypertrophy: are they relevant for clinical applications in humans? *J Orthop Sports Phys Ther* 32: 36–43, 2002. doi:10.2519/jospt.2002.32.2.36.
32. **Frontera WR**, **Ochala J.** Skeletal muscle: a brief review of structure and function. *Calcif Tissue Int* 96: 183–195, 2015. doi:10.1007/s00223-014-9915-y.
33. **Michaud SE**, **Ménard C**, **Guy L-G**, **Gennaro G**, **Rivard A.** Inhibition of hypoxia-induced angiogenesis by cigarette smoke exposure: impairment of the HIF-1alpha/VEGF pathway. *FASEB J* 17: 1150–1152, 2003. doi:10.1096/fj.02-0172fje.
34. **Cielen N**, **Heulens N**, **Maes K**, **Carmeliet G**, **Mathieu C**, **Janssens W**, **Gayan-Ramirez G.** Vitamin D deficiency impairs skeletal muscle function in a smoking mouse model. *J Endocrinol* 229: 97–108, 2016. doi:10.1530/JOE-15-0491.
35. **Dirks-Naylor AJ**, **Lennon-Edwards S.** The effects of vitamin D on skeletal muscle function and cellular signaling. *J Steroid Biochem Mol Biol* 125: 159–168, 2011. doi:10.1016/j.jsbmb.2011.03.003.
36. **Domingues-Faria C**, **Chanet A**, **Salles J**, **Berry A**, **Giraudet C**, **Patrac V**, **Denis P**, **Bouton K**, **Goncalves-Mendes N**, **Vasson M-P**, **Boirie Y**, **Walrand S.** Vitamin D deficiency down-regulates Notch pathway contributing to skeletal muscle atrophy in old wistar rats. *Nutr Metab (Lond)* 11: 47, 2014. doi:10.1186/1743-7075-11-47.
37. **Janssens W**, **Bouillon R**, **Claes B**, **Carremans C**, **Lehouck A**, **Buysschaert I**, **Coolen J**, **Mathieu C**, **Decramer M**, **Lambrechts D.** Vitamin D deficiency is highly prevalent in COPD and correlates with variants in the vitamin D-binding gene. *Thorax* 65: 215–220, 2010. doi:10.1136/thx.2009.120659.
38. **Girgis CM**, **Clifton-Bligh RJ**, **Hamrick MW**, **Holick MF**, **Gunton JE.** The roles of vitamin D in skeletal muscle: Form, function, and metabolism. *Endocr Rev* 34: 33–83, 2013. doi:10.1210/er.2012-1012.
39. **Cutillas-Marco E**, **Fuertes-Prosper A**, **Grant WB**, **Morales-Suárez-Varela M.** Vitamin D deficiency in South Europe: effect of smoking and aging. *Photodermatol Photoimmunol Photomed* 28: 159–161, 2012. doi:10.1111/j.1600-0781.2012.00649.x.
40. **Hermann AP**, **Brot C**, **Gram J**, **Kolthoff N**, **Mosekilde L.** Premenopausal smoking and bone density in 2015 perimenopausal women. *J Bone Miner Res* 15: 780–787, 2010. doi:10.1359/jbmr.2000.15.4.780.
41. **Lange NE**, **Sparrow D**, **Vokonas P**, **Litonjua AA.** Vitamin D deficiency, smoking, and lung function in the normative aging study. *Am J Respir Crit Care Med* 186: 616–621, 2012. doi:10.1164/rccm.201110-1868OC.
42. **Heulens N**, **Korf H**, **Cielen N**, **De Smidt E**, **Maes K**, **Gysemans C**, **Verbeken E**, **Gayan-Ramirez G**, **Mathieu C**, **Janssens W.** Vitamin D deficiency exacerbates COPD-like characteristics in the lungs of cigarette smoke-exposed mice. *Respir Res* 16: 110, 2015. doi:10.1186/s12931-015-0271-x.
43. **Johnson LE**, **DeLuca HF.** Reproductive defects are corrected in vitamin D-deficient female rats fed a high calcium, phosphorus and lactose diet. *J Nutr* 132: 2270–2273, 2002. doi:10.1093/jn/132.8.2270.
44. **Serré J**, **Mathyssen C**, **Ajime TT**, **Korf H**, **Maes K**, **Heulens N**, **Gysemans C**, **Mathieu C**, **Vanaudenaerde B**, **Janssens W**, **Gayan-Ramirez G.** Airway infection with nontypeable Haemophilus influenzae is more rapidly eradicated in vitamin D deficient mice. *J Steroid Biochem Mol Biol* 187: 42–51, 2019. doi:10.1016/j.jsbmb.2018.10.021.
45. **Thomas D**, **Maes K**, **Agten A**, **Heunks L**, **Dekhuijzen R**, **Decramer M**, **Van Hees H**, **Gayan-Ramirez G.** Time course of diaphragm function recovery after controlled mechanical ventilation in rats. *J Appl Physiol* 115: 775–784, 2013. doi:10.1152/japplphysiol.00302.2012.
46. **Paepe B**, **Brusselle GG**, **Maes T**, **Creus KK**, **D'hose S**, **D'Haese N**, **Bracke KR**, **D'hulst AI**, **Joos GF**, **Bleecker JL.** TNFα receptor genotype influences smoking-induced muscle-fibre-type shift and atrophy in mice. *Acta Neuropathol* 115: 675–681, 2008. doi:10.1007/s00401-008-0348-4.
47. **Rinaldi M**, **Maes K**, **De Vleeschauwer S**, **Thomas D**, **Verbeken EK**, **Decramer M**, **Janssens W**, **Gayan-Ramirez GN.** Long-term nose-only cigarette smoke exposure induces emphysema and mild skeletal muscle dysfunction in mice. *Dis Model Mech* 5: 333–341, 2012. doi:10.1242/dmm.008508.
48. **Cielen N**, **Maes K**, **Heulens N**, **Troosters T**, **Carmeliet G**, **Janssens W**, **Gayan-Ramirez GN.** Interaction between physical activity and smoking on lung, muscle and bone in mice. *Am J Respir Cell Mol Biol* 54: 674–682, 2015. doi:10.1165/rcmb.2015-0181OC.
49. **Yang A**, **Lv Q**, **Chen F**, **Wang Y**, **Liu Y**, **Shi W**, **Liu Y**, **Wang D.** The effect of vitamin D on sarcopenia depends on the level of physical activity in older adults. *J Cachexia Sarcopenia Muscle* 11: 678–689, 2020. doi:10.1002/jcsm.12545.
50. **Montes De Oca M**, **Loeb E**, **Torres SH**, **De Sanctis J**, **Hernández N**, **Tálamo C.** Peripheral muscle alterations in non-COPD smokers. *Chest* 133: 13–18, 2008. doi:10.1378/chest.07-1592.
51. **Bhat M**, **Kalam R**, **Qadri SS**, **Madabushi S**, **Ismail A.** Vitamin D deficiency-induced muscle wasting occurs through the ubiquitin proteasome pathway and is partially corrected by calcium in male rats. *Endocrinology* 154: 4018–4029, 2013. doi:10.1210/en.2013-1369.
52. **Ceglia L**, **Rivas DA**, **Pojednic RM**, **Price LL**, **Harris SS**, **Smith D**, **Fielding RA**, **Dawson-Hughes B.** Effects of alkali supplementation and vitamin D insufficiency on rat skeletal muscle. *Endocrine* 44: 454–464, 2013. doi:10.1007/s12020-013-9976-0.
53. **Mithal A**, **Bonjour JP**, **Boonen S**, **Burckhardt P**, **Degens H**, **El Hajj Fuleihan G**, **Josse R**, **Lips P**, **Morales Torres J**, **Rizzoli R**, **Yoshimura N**, **Wahl DA**, **Cooper C**, **Dawson-Hughes B**; **IOF CSA Nutrition Working Group.** Impact of nutrition on muscle mass, strength, and performance in older adults. *Osteoporos Int* 24: 1555–1566, 2013 [Erratum in *Osteoporos Int* 24: 1527–1528, 2013]. doi:10.1007/s00198-012-2236-y.
54. **Armstrong RB**, **Marum P**, **Tullson P**, **Saubert CW IV.** Acute hypertrophic response of skeletal muscle to removal of synergists. *J Appl Physiol Respir Environ Exerc Physiol* 46: 835–842, 1979. doi:10.1152/jappl.1979.46.4.835.
55. **Thompson RW**, **McClung JM**, **Baltgalvis KA**, **Davis JM**, **Carson JA.** Modulation of overload-induced inflammation by aging and anabolic steroid administration. *Exp Gerontol* 41: 1136–1148, 2006. doi:10.1016/j.exger.2006.08.013.
56. **Kandarian SC**, **White TP.** Mechanical deficit persists during long-term muscle hypertrophy. *J Appl Physiol (1985)* 69: 861–867, 1990. doi:10.1152/jappl.1990.69.3.861.
57. **Bodine SC**, **Stitt TN**, **Gonzalez M**, **Kline WO**, **Stover GL**, **Bauerlein R**, **Zlotchenko E**, **Scrimgeour A**, **Lawrence JC**, **Glass DJ**, **Yancopoulos GD.** Akt/mTOR pathway is a crucial regulator of skeletal muscle hypertrophy and can prevent muscle atrophy in vivo. *Nat Cell Biol* 3: 1014–1019, 2001. doi:10.1038/ncb1101-1014.
58. **Stienen GJM**, **Kiers JL**, **Bottinelli R**, **Reggiani C.** Myofibrillar ATPase activity in skinned human skeletal muscle fibres: fibre type and temperature dependence. *J Physiol* 493: 299–307, 1996. doi:10.1113/jphysiol.1996.sp021384.
59. **Sandri M**, **Sandri C**, **Gilbert A**, **Skurk C**, **Calabria E**, **Picard A**, **Walsh K**, **Schiaffino S**, **Lecker SH**, **Goldberg AL.** Foxo transcription factors induce the atrophy-related ubiquitin ligase atrogin-1 and cause skeletal muscle atrophy. *Cell* 117: 399–412, 2004. doi:10.3109/10715762.2014.904507.
60. **Walters TJ**, **Sweeney HL**, **Farrar RP.** Influence of electrical stimulation on a fast-twitch muscle in aging rats. *J Appl Physiol (1985)* 71: 1921–1928, 1991. doi:10.1152/jappl.1991.71.5.1921.
61. **Oliveira JRS**, **Mohamed JS**, **Myers MJ**, **Brooks MJ**, **Alway SE.** Effects of hindlimb suspension and reloading on gastrocnemius and soleus muscle mass and function in geriatric mice. *Exp Gerontol* 115: 19–31, 2019. doi:10.1016/j.exger.2018.11.011.